Impact fragmentation of an ideal brittle crystal

Yoshinori Hayakawa
Research Institute of Electrical Communication, Tohoku University, Katahira, Aoba-ku, Sendai 980-77, Japan
(Received 6 November 1995)

A deterministic model of fragmentation of a brittle crystal is presented. In the modeling, dynamics of a viscoelastic material is taken into account, though inhomogeneity in material and interactions between fragments are totally neglected to reduce computational costs. By numerical simulations for impulsive loadings, we analyze the processes during fragmentation, and find that a power-law mass distribution of fragments emerges insensitively to material specific parameters. Assuming a finite-size scaling form of the mass distribution function, we present an expression for the exponent of mass distribution, which gives agreement with numerical results and experimental data. [S0163-1829(96)03021-4]

I. INTRODUCTION

Fragmentation of brittle material caused by pulse loading is often seen in many areas of science and technology ranging from material design to cosmology. The characteristics and statistics of resultant fragments have been studied so far to find a general law of this very complicated phenomena. One of the most intensively investigated properties at fragmentation is its size or mass distribution function. Depending on experimental conditions and kinds of specimen, several types of distribution functions, including exponential,[1] log normal,[2] and power law,[3,4] are used to give a representation of data. In particular, a power-law form of mass distribution is known to be applicable to many cases of impact fragmentation, such as spallation of rocks,[4–6] ices,[7] and glasses,[3] and there seems to exist some universality.[8,9] On the other hand, little direct observation has been made because of the very limited capability of measurement, and consequently the detail mechanisms which give rise to such distribution functions, especially power-law distribution, is also little understood.

In this paper, we first introduce a model of dynamic fracture by using an ideal brittle crystal as a ''specimen'' subject to impulsive load. Then we analyze the process of breakage and the statistics of fragments for several conditions by numerical simulations. Finally, we present a scaling argument based on the numerical results, and propose an expression of the exponent for power-law distribution in agreement with numerical and other experimental results.

II. MODEL

Fragmentation of brittle material is, in general, supposed to consist of several complicated processes in microscopic scale. By impulsive loads, localized deformation propagates in medium with scattering and reflection according to microstructure of material, such as microflaws and grain boundaries. If the deformation is large, the elastic property of the material might become nonlinear and modes of vibration will couple. Formation of a crack takes place accompanied with plasticity near crack tips and coalescence of crack faces.[10]

In order to clarify what are the relevant factors to the emergence of robust statistics like a power-law mass distribution at fragmentation, we make a simplification which may not be applied to real materials. For instance, in this study, we do not take into account any inhomogeneity and plasticity of material. Furthermore the evolution of the system obeys a Newton equation of motion and a deterministic rule of breakage rather than stochastic modeling.[11] On the other hand, dynamics of a viscoelastic material is fully considered.

Let us give a detailed description of the present model. The model material is a simple cubic crystal of lattice constant a_1. Atoms in nearest neighbors (NN) and next-nearest neighbors (NNN) are binded with ideal Hook springs, which can be rotated freely around the atom [see Fig. 1]. Thus, in the equilibrium configuration, natural length of NNN bond is $a_2=\sqrt{2}a_1$. Here we denote k_1 as the spring constant for NN bonds and k_2 for NNN bonds. The NNN interaction is essential for representation of elastic objects, since shear stress only appears when $k_2>0$. Yielded stress is a linear function of strain if the deformation is small. But, if not, one should note that nonlinear elasticity comes out even with ideal Hookean springs.

The force applied to the atom with index i is represented by

$$\mathbf{F}_i=\sum_{j\in \mathrm{NN}} k_1 \frac{\mathbf{r}_i-\mathbf{r}_j}{|\mathbf{r}_i-\mathbf{r}_j|}\,(a_1-|\mathbf{r}_i-\mathbf{r}_j|)$$

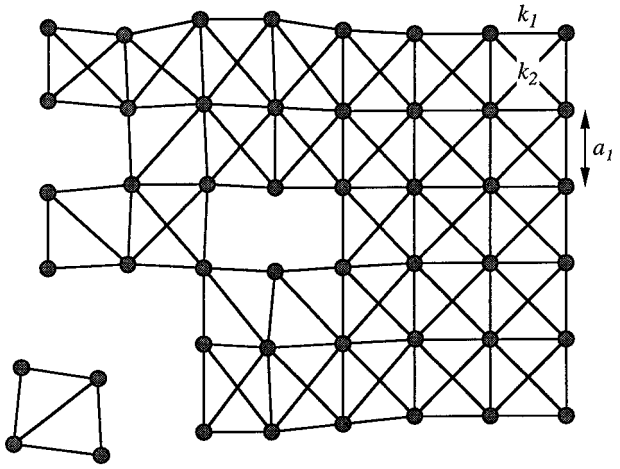

FIG. 1. Schematic diagram of the present model: Model crystal with NN and NNN interactions.

$$+\sum_{j\in \mathrm{NNN}} k_2 \frac{\mathbf{r}_i-\mathbf{r}_j}{|\mathbf{r}_i-\mathbf{r}_j|}(a_2-|\mathbf{r}_i-\mathbf{r}_j|). \quad (1)$$

Using $\mathbf{F}_i$, the equation of motion for ith atom is given by

$$\ddot{\mathbf{r}}_i=-\gamma\sum_{j\in \frac{\mathrm{NN}}{\mathrm{NNN}}}(\dot{\mathbf{r}}_1-\dot{\mathbf{r}}_j)+\mathbf{F}_i+\mathbf{F}_i^{\mathrm{ext}}, \quad (2)$$

where γ is the parameter of dissipation rate and $\mathbf{F}^{\mathrm{ext}}$ is an external force. For simplicity, every atom has the same mass ($m=1$). In our simulations, the dissipation rate γ is taken to be small enough so that characteristic relaxation time m/γ is at least larger than whole simulation time.

Next we introduce a simple criterion of failure, as used in the precedent study of quasistatic crack propagation.[12] At every time step, deformation of each spring is calculated. If a spring has a expansion rate $\delta r/a$ larger than threshold value $u^{\max}=\delta r^{\max}/a$, the spring constant of the corresponding bond changes to zero. This process is irreversible, and neither reconnection nor rearrangement of atoms is allowed. In the following computer simulations, we took $a_1=1$ and $u^{\max}=0.1$, if not specified.

In the fragmentation processes, the time scale of crack formation is comparable to that of sound propagation. On the other hand, the velocity of pieces of fragments is, in general, quite smaller than that of sound. Thus we can expect that fragmentation processes can be virtually divided into two stages with different time scales, that is, creation of cracks and collision of fragments. In this study, we separate these and mostly focus on the former process. That is, we neglect every secondary interaction between atoms, such as collision of fragments, indentation, and coalescence at crack faces. By this simplification computational time can be significantly reduced.

Here we summarize some material specific parameters.[13] Taking the continuum limit of the equation of motion, one can find that the velocity of a planer wave in the (100) direction is $v_l=\sqrt{c_1/\rho}$ for the longitudinal mode, and $v_t=\sqrt{c_2/\rho}$ for the transversal mode, where $c_1=(k_1+2k_2)/a_1$ and $c_2=k_2/a_1$. Young's modulus E is

$$E=\frac{(c_1-c_2)(c_1+2c_2)}{c_1+c_2}, \quad (3)$$

and Poisson ratio σ is

$$\sigma=\frac{c_2}{c_1+c_2}, \quad (4)$$

for the (100) direction, respectively. In the following analysis, $k_1=k_2=5$ are used. Since the elasticity of the model crystal is inherently anisotropic, these parameters can vary as a function of the direction of loading within the order of unity.

III. NUMERICAL SIMULATIONS

As an initial condition, the configuration of atoms is set to be at slightly different positions from equilibrium by using Gaussian-distributed random numbers. The velocity of each atom also has small initial Gaussian deviations from zero at $t=0$. The model crystal subject to loading has typical dimensions from $20\times20\times20$ up to $33\times33\times33$, and several different aspect ratios of the specimen are examined, too.

Although fragmentation takes place in various situations in nature, in this study, we focus on the following types of impulsive loadings:

Case I: Impact at a side of a cubic crystal. To gain the amount of momentum transfer into the crystal, a few layers of atoms from the surface are also subjected to the impact. In this case, the atoms near the surface sites have a load pushing the crystal in a primary axis, say the z axis, during a short period. Starting the process at $t=0$, the applied force is a linear function of time with a cutoff t_c as

$$F^{\mathrm{ext}}(\mathrm{surface})=\begin{cases} f_0 t, & t<t_c \\ 0, & t>t_c, \end{cases}$$

where $f_0=4$ and $t_c=5$ in typical runs of simulations. By this method, the energy injected to the crystal cannot be specified explicitly.

Case II: Repetitive bouncing on a plane. This is a very simplified modeling such that a material falls by gravitational force onto an elastic wall. The specimen is accelerated by a constant force $F_{\mathrm{ext}}=-g$ in the z direction. . Atoms crossing down to threshold height, e.g., ground level z_c, the atoms feel harmonic repulsive force represented by

$$F^{\mathrm{ext}}(\mathrm{surface})=\begin{cases} k_{\mathrm{wall}}(z_c-z)-g, & z<z_c, \\ -g, & z>z_c, \end{cases}$$

and they are pushed back. Typical values of parameters are $k_{\mathrm{wall}}=10$, $g=0.04$. Fragments bounce on the ground repeatedly, and for finite γ, the motion will eventually stop. The equation of motion is solved with a second-order Runge-Kutta scheme. The typical time difference Δt is 0.001.

IV. FRAGMENTATION PROCESS

For strong enough impulsive loading, a model brittle crystal entirely breaks into fragments as shown in Fig. 2. In order to examine the distribution and propagation of spallation activity, we make a plot of the position of the crack nucleation site as a function of time as shown in Fig. 3. As seen in the figure, a localized nucleation zone propagates with a constant velocity nearly equal to the sound velocity v_l in longitudinal mode. In our model, despite no initial flaw being introduced, the ''microcrack'' is produced spontaneously by local strong deformation of the crystal. It is known that the velocity of Rayleigh wave v_R, which is fairly smaller than v_l, gives the limit of the propagation speed of a single crack.[14] Therefore, we can expect that, behind the active zone, some of the nucleated cracks grow and percolate each other in a slower time scale than the wave propagation. When the density wave reaches the end of a specimen, a large volume of the sample exfoliates probably because the amplitude of the wave is enhanced by reflection on the boundary.

To characterize the stages of the breakage process and its activity, we make a plot of the number of broken bonds per unit time as a function of time (Fig. 4). There are three apparent regimes in the breakage: (i) first peak which corresponds to the initial impulse load, (ii) the intermediate stage when the density wave propagates through the material with high breaking rate, and (iii) the final stage with a low break-

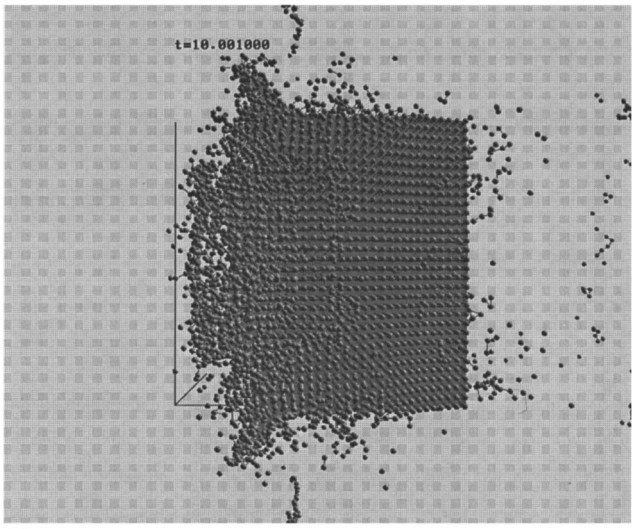

(a)

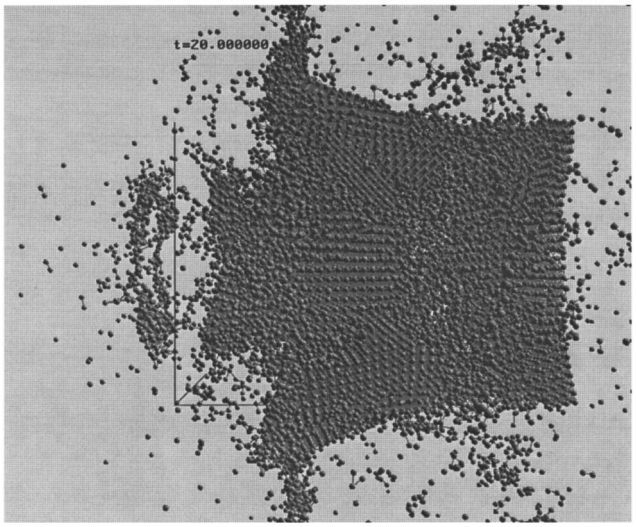

(b)

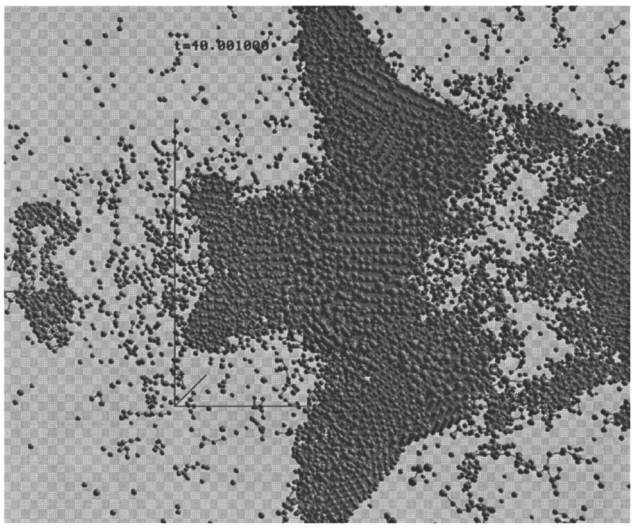

(c)

FIG. 2. Three-dimensional view of a fragmentation process. The crystal consists of 32×32×32 atoms. The left side of the cube is subject to initial impact. (a) $t=10$, (b) $t=20$, (c) $t=40$.

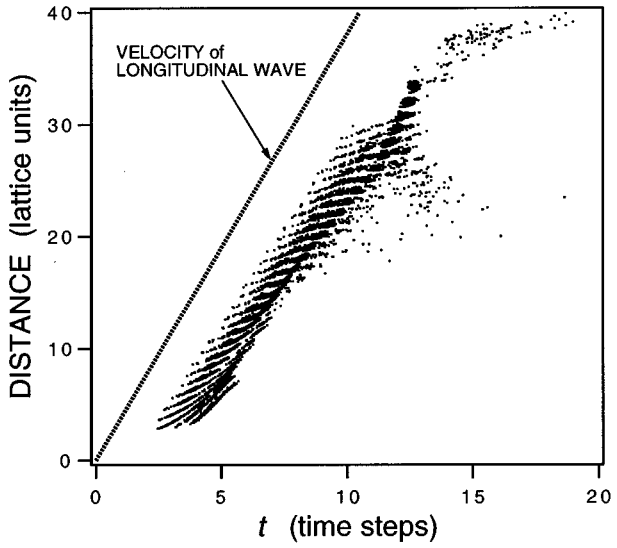

FIG. 3. Position of crack nucleation along with the direction of shock propagation (z) as a function of time.

age rate after the wave reaches the other end of the specimen. Between (ii) and (iii), a large peak is seen corresponding to the first arrival of the wave at the other side of the specimen.

Breakage mostly takes place in stage (i) and (ii), and the rate decays slowly with time in (iii). From the visualization of computer simulations, it is seen that formation of the crack is almost completed during stage (ii) and in stage (iii) larger fragments scatter into space. In Fig. 4(b), the rate is shown in logarithmic scale as a function of time. In the plot, the origin of time is taken to be at the second large peak of the breakage rate [t_1 in Fig. 4(a)]. The decay is approximately characterized by a power-law decay $n_b \sim t^{-\alpha}$ with $\alpha=1.5\sim2$. The slow dynamics is considered as a relaxation process in which segments produced in stage (i) and (ii) come apart by cutting bridging bonds over the segments. The relation between fragment structure and the dynamics in stage (iii) is our future problem.

V. FRAGMENT MASS DISTRIBUTION

Cumulative mass distribution has been often used for characterization of fragmentation experiments. Let $n(m)$ be the distribution function of fragments of mass m, the cumulative distribution function is defined as

$$N(m)=\int_m^\infty n(m')dm'. \tag{5}$$

In data processing, we first sort resultant fragments by mass (i.e., number of atoms) in descending order and make a histogram as usually done in experiments.

When the initial deformation is symmetric, the resulting cumulated mass distribution has some steps in it due to several same-size fragments. In order to obtain better statistics within a limited system size, we have tested several kinds of conditions. From the observation of numerical results, asymmetry of specimen and initial randomness lead to some improvement of statistics. However, the tendency of the mass distribution function seems to be robust against such effects.

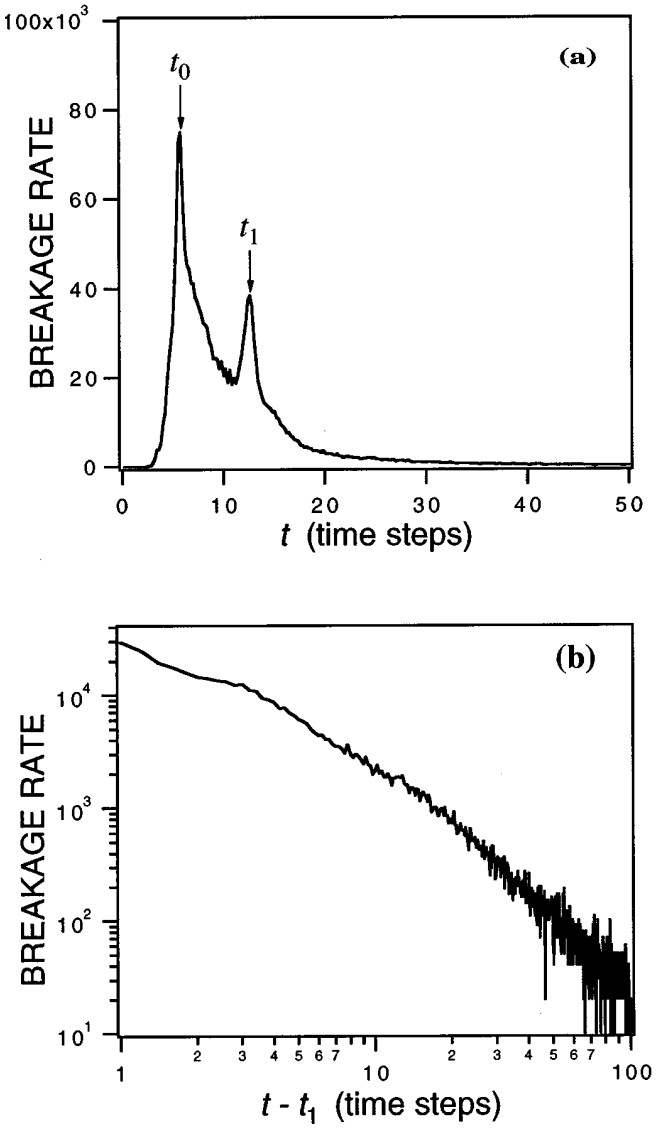

FIG. 4. Number of broken bonds per unit time as a function of time. (a) A linear scale plot, (b) a log-log plot in relaxation regime.

In Fig. 5, a typical cumulative mass distribution is shown for several different time steps. As fragmentation proceeds, the form of distribution changes. After a long enough time, typically ten times longer than the time required for wave propagation through specimens, the breakage almost finishes and the distribution becomes frozen. In the final stage, there are two typical regions in the distribution function: one is the power-law region which is described as

$$N(m) \sim m^{-b}, \tag{6}$$

for large fragment mass, and the other is a small mass region showing apparently a larger decay rate. The crossover between those two regions is seen at $m \simeq 10$. For large size fragments the least-squares fitting of the data gives $b = 0.64 \pm 0.02$, which is in agreement with three-dimensional experimental results.[8] From several independent simulations for different initial conditions and material specific parameters, we found that the value of b is very robust and distributed around 2/3.

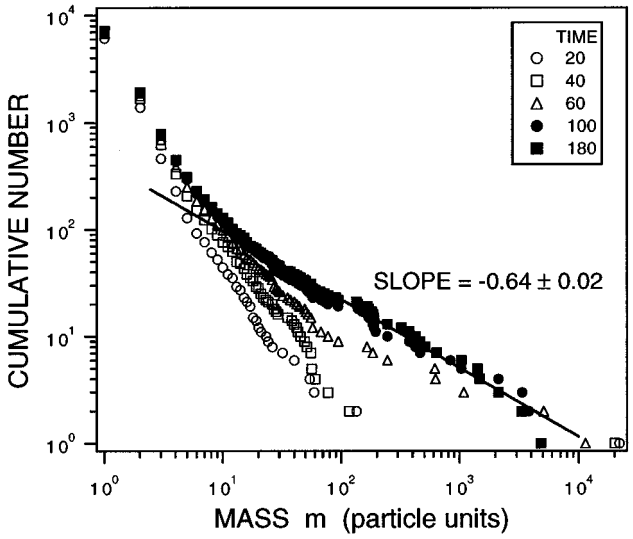

FIG. 5. Typical cumulative mass distribution of fragments produced by one-time impulsive load. The crystal is 23×33×41 in dimension.

In order to examine what the crossover in mass distribution implies, we measure the mass-size relation at a late stage of fragmentation (Fig. 6). Here we estimate the typical size of fragments with the radius of gyration r_g. For large scale, fragments can be regarded as three-dimensional solid objects rather than complex substances like fractals,[15] because points in the plot approximately lie on a curve represented by $r_g \sim m^{1/3}$. On the other hand, for smaller size <10, geometry of fragments change from a three-dimensional to a stringy form as a chain molecule. That is, the crossover is seen corresponding to the change of dimensionality of fragments, and it will disappear as the system size becomes larger.

Contrary to the fragmentation with single pulse loading, repeated impact (Case II) causes another mass distribution. When the number of bouncing is small, the distribution func-

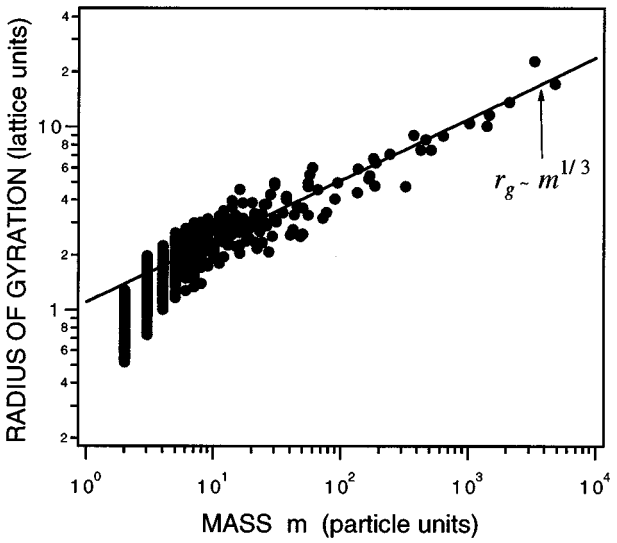

FIG. 6. Mass-size relation of resultant fragments obtained by the same simulation as Fig. 5.

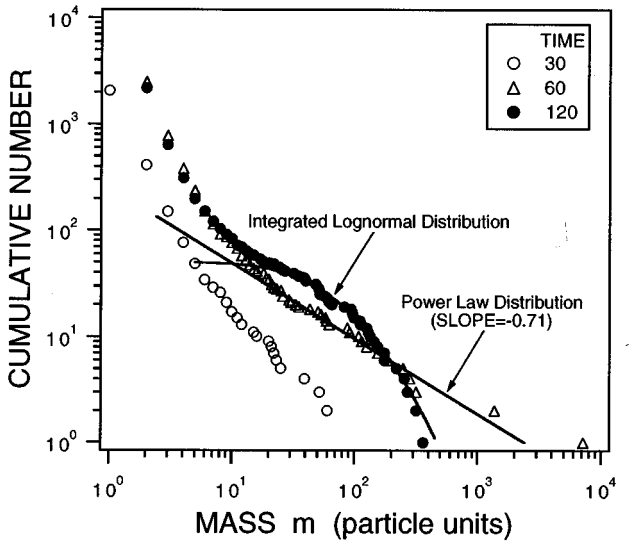

FIG. 7. Typical cumulative mass distribution for repetitive loads by bouncing on an elastic wall. The size of the crystal is 32×32 ×32.

tion seems to approach a power-law form. However, as bouncing proceeds, the tail of the distribution falls gradually, and finally no power-law region is seen for large size fragments as shown in Fig. 7. The solid line in Fig. 7 represents an integrated log normal distribution function

$$N_{\ln}(m)=A\int_m^{\infty}\frac{\exp(-[\ln(m'/\overline{m})]^2/2\sigma^2)}{(2\pi\sigma^2)^{1/2}m'}\,dm' \qquad (7)$$

with the parameters $(A,\overline{m},\sigma)$ to fit the data. The numerical results at the late stage can be well fit with a log normal distribution. This indicates that the fragmentation by repetitive loadings can be regarded as a stochastic multiplicative process.[2,16] Furthermore, it is expected that secondary collision between fragments or collision with external boundaries may change the mass distribution from a power law to rounded form in log-log plots.

VI. DISCUSSION

Let us derive phenomenologically the expression of b by the scaling argument based on the numerical observation. In numerical evidence, the nucleation of a crack occurs mostly on the planer front moving at a constant velocity, and the partitioning of the material is almost completed in the region where the wave passed, except some bridges between segments. Since the system obeys a wave-type equation, the distance L between wave front and impact point (or plane) is the only macroscopic characteristic length if the size of the specimen is large enough. In fact, other microscopic details of the material, such as the lattice structure of length scale a_1, is thought to be irrelevant for large scale fragmentation processes in our model. Furthermore, impulsive external loads do not yield a characteristic wavelength inside the specimen except a microscopic cutoff wavelength.

Taking these into account, we assume the following two-exponent scaling form[15] of the mass distribution function:

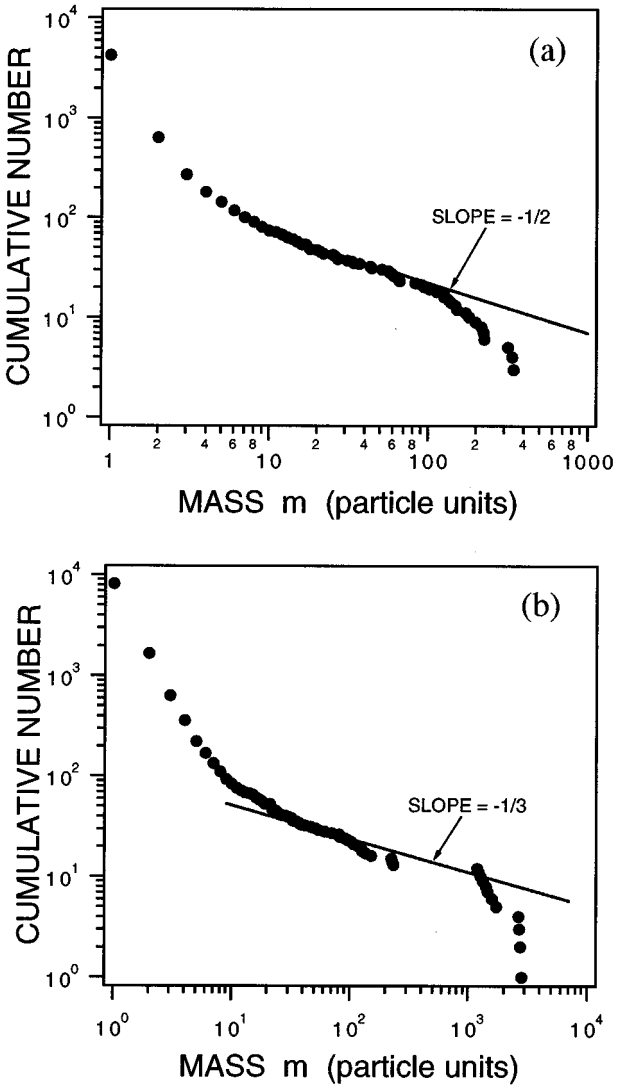

FIG. 8. Cumulative mass distribution for some different conditions: (a) Two-dimensional fragmentation by impulsive load from one side of the square crystal (200×200), (b) three-dimensional fragmentation initiated by sudden expansion of the cylindrical region at the center of the cubic crystal (33×33×33).

$$n(m,L)\sim m^{-\beta}f(L/m^{\gamma}), \qquad (8)$$

where $f(x)$ is a function which gives $f(x)=0$ for large x. From the definition of the cumulative distribution function, $b=\beta-1$. If resulting fragments have a simple shape with size-mass relation $l\sim m^{1/d}$, which is suggested by the mass-size relation shown in Fig. 6, we expect $\gamma=1/d$ in the scaling function, where d is the dimension of space.

Using $n(m,L)$, total mass $M(L)$ within ''thickness'' of L can be represented by

$$M(L)=\int_0^{\infty}mn(m,L)dm. \qquad (9)$$

This can be simply reduced to $M(L)=CL^{d(2-\beta)}$ where C is a constant independent of L.

On the other hand, $M(L)\sim L$ has to be held for planer wave propagation so as to conserve total mass, one can therefore obtain

$$\beta=2-\gamma=2-1/d. \tag{10}$$

This simple expression for β gives good agreement with experimental results of three-dimensional impact fragmentation as well as our numerical results. As long as the finite-size scaling of Eq. (8) is held, the value of β should be independent of other details of the material.

By a similar discussion, in three-dimensional geometry, we expect that a cylindrical wave front leads to mass distribution with $\beta=4/3$, because $M(L)\sim L^2$. For spherical wave cases, that is, for pointlike initial deformation, $\beta=1$ for any dimension of space. In experiments using many kinds of materials, e.g., rocks, it is known that b may take different values depending on experimental conditions such as obstacle size. We expect that dimensionality of the specimen and the shape of the wave front will cause the scatter or crossover[17] of b in real systems.

In order to test Eq. (10) for other geometry and dimension of space, we carried out further numerical simulations in the following cases: (i) a two-dimensional square lattice subject to homogeneous impact from one side (i.e., a planer wave front in two dimensions), and (ii) a three-dimensional cubic lattice to which sudden radial dilation along a central axis is applied (i.e., a cylindrical wave front in three dimensions). In Fig. 8, the resulting data of mass distribution are shown. For two-dimensional cases, β is evidently smaller than that for three-dimensional cases, and $b=\beta-1\simeq 1/2$ for large fragments [Fig. 8(a)]. For a cylindrical wave front in three dimensions, $b\simeq 1/3$ gives better representation to the numerical result in a certain range of fragment size [Fig. 8(b)]. We therefore conclude that both data agree with our derivation, while quantitative and systematic analysis has to be made in a future study. These results suggest that one might obtain the information about the dynamical process inside the material from the value of the exponent obtained by experiments.

VII. CONCLUSION

We present a simple deterministic model of fragmentation of brittle material, in which healing of cracks and secondary collisions of produced fragments are not taken into account. By the three-dimensional computer simulations, direct observation of fragmentation processes is made. In the initial stage of the process, failure takes places mostly near the wave front of deformation and a complex structure of crack forms. After the wave reaches the other end of the specimen, larger fragments start scattering into space with breaking bridge bonds between pieces, accordingly the total rate of microfailure decays in a power-law form. The cumulative mass distribution function has a crossover between small and large fragment sizes due to the changes of shapes. For the large scale, a power-law distribution with exponent nearly 2/3, which agrees well with experiments, is obtained, even though the size of the sample specimen is very limited. Those numerical results imply that the power-law mass distribution found in impact fragmentation is originated not from inhomogeneity of materials but from a dynamical process of crack formation during density wave propagation.

From a scaling argument based on numerical observations, we obtained the expression of the exponent $\beta(=b+1)$ of the mass distribution function as $\beta=2-1/d$. When the initial deformation propagates on a cylindrical surface, we expect $\beta=3/4$. Our computer simulations give consistent results with these expressions.

ACKNOWLEDGMENTS

We acknowledge helpful discussions with Professor M. Sano, Professor H. Takayasu, and Professor Y. Sawada. Part of this work was supported by the Japanese Grant-in-Aid for Science Research Fund from the Ministry of Education, Science, and Culture (No. 0740500, No. 05232102).

[1] D. E. Grady and M. E. Kipp, J. Appl. Phys. **58**, 1210 (1985).
[2] A. N. Kolmogoroff, Dokl. Acad. Nauk SSSR **31**, 99 (1941).
[3] J. J. Gilvarry and B. H. Bergstrom, J. Appl. Phys. **32**, 400 (1961).
[4] W. K. Hartmann, Icarus **10**, 201 (1969).
[5] A. Fujiwara, G. Kamimoto, and A. Tsukamoto, Icarus **31**, 277 (1977).
[6] T. Matsui, T. Waza, K. Kani, and S. Suzuki, J. Geophys. Res. **87**, B13, 10 968 (1982).
[7] M. Kato, Y. Iijima, M. Arakara, Y. Okimura, A. Fujimura, N. Maeno, and H. Mizutani, Icarus **113**, 423 (1995).
[8] L. Oddershede, P. Dimon, and J. Bohr, Phys. Rev. Lett. **71**, 3107 (1993).
[9] H. Inaoka and H. Takayasu, Fractals (to be published).
[10] B. Lawn, *Fracture of Brittle Solids*, 2nd ed. (Cambridge University Press, Cambridge, 1993).
[11] *Statistical Models for the Fracture in Disordered Media*, edited by H. J. Herrmann and S. Roux (North-Holland, Amsterdam, 1990).
[12] Y. Hayakawa, Phys. Rev. E **49**, R1804 (1994).
[13] L. D. Landau and E. M. Lifshitz, *Theory of Elasticity* (Pergamon, New York, 1959).
[14] L. B. Freund, *Dynamic Fracture Mechanics* (Cambridge University Press, New York, 1990).
[15] T. Vicsek, *Fractal Growth Phenomena*, 2nd ed. (World Scientific, Singapore, 1991).
[16] T. Ishii and M. Matsushita, J. Phys. Soc. Jpn. **61**, 3474 (1992).
[17] Y. Takagi, H. Mizutani, and S. Kawakami, Icarus **59**, 462 (1984).